Supplement of Atmos. Chem. Phys., 21, 9719–9739, 2021
https://doi.org/10.5194/acp-21-9719-2021-supplement


Atmospheric Chemistry and Physics
Open Access

*Supplement of*

# Disparities in particulate matter ($PM_{10}$) origins and oxidative potential at a city scale (Grenoble, France) – Part 2: Sources of $PM_{10}$ oxidative potential using multiple linear regression analysis and the predictive applicability of multilayer perceptron neural network analysis

**Lucille Joanna S. Borlaza et al.**

*Correspondence to:* Lucille Joanna S. Borlaza (lucille-joanna.borlaza@univ-grenoble-alpes.fr) and Gaëlle Uzu (gaelle.uzu@ird.fr)

**Table of Contents:**



## S1. PM characterization

**Table S1. Annual average of $PM_{10}$ mass concentrations and chemical compositions (in µg $m^{-3}$) at all sites, and individual urban sites in Grenoble, France.**

| Species | Unit | Mean [Q1, Q3] | | | |
|---|---|---|---|---|---|
| | | All sites | CB (urban hyper-center) | LF (urban background) | Vif (peri-urban) |
| PM10recons | µg/m³ | 14.4 [8.0, 17.8] | 16.0 [8.8, 20.3] | 14.2 [8.1, 17.2] | 13.1 [7.3, 16.5] |
| OC* | | 3.95 [2.28, 5.0] | 4.14 [2.43, 5.28] | 3.95 [2.28, 4.73] | 3.75 [2.12, 4.49] |
| EC | | 1.01 [0.46, 1.32] | 1.18 [0.57, 1.5] | 1.12 [0.53, 1.35] | 0.73 [0.34, 0.85] |
| $Cl^-$ | | 0.12 [0.01, 0.1] | 0.16 [0.02, 0.15] | 0.08 [0.01, 0.08] | 0.1 [0.0, 0.08] |
| $NO_3^-$ | | 2.02 [0.48, 2.11] | 2.55 [0.67, 3.16] | 1.78 [0.51, 1.7] | 1.72 [0.36, 1.7] |
| $SO_4^{2-}$ | | 1.48 [0.81, 1.89] | 1.58 [0.89, 2.0] | 1.53 [0.87, 1.97] | 1.33 [0.69, 1.74] |
| $Na^+$ | | 0.17 [0.07, 0.2] | 0.2 [0.08, 0.24] | 0.15 [0.06, 0.19] | 0.15 [0.06, 0.18] |
| $NH_4^+$ | | 0.85 [0.3, 0.89] | 0.99 [0.31, 1.11] | 0.81 [0.32, 0.81] | 0.75 [0.27, 0.79] |
| $K^+$ | | 0.15 [0.07, 0.18] | 0.16 [0.08, 0.19] | 0.15 [0.07, 0.17] | 0.13 [0.06, 0.17] |
| $Mg^{2+}$ | | 0.02 [0.01, 0.02] | 0.02 [0.01, 0.03] | 0.02 [0.01, 0.02] | 0.02 [0.01, 0.02] |
| $Ca^{2+}$ | | 0.32 [0.13, 0.44] | 0.36 [0.13, 0.52] | 0.31 [0.12, 0.38] | 0.3 [0.13, 0.42] |
| MSA | | 0.02 [0.01, 0.03] | 0.03 [0.01, 0.03] | 0.02 [0.01, 0.03] | 0.02 [0.01, 0.03] |
| Levoglucosan | | 0.3 [0.02, 0.42] | 0.25 [0.02, 0.35] | 0.28 [0.02, 0.42] | 0.36 [0.02, 0.47] |
| Mannosan | | 0.03 [0.0, 0.04] | 0.03 [0.0, 0.04] | 0.03 [0.0, 0.05] | 0.04 [0.0, 0.05] |
| Polyols | | 0.04 [0.01, 0.06] | 0.04 [0.01, 0.06] | 0.04 [0.01, 0.06] | 0.05 [0.01, 0.07] |
| Cellulose | | 0.08 [0.02, 0.12] | 0.13 [0.07, 0.17] | 0.05 [0.02, 0.08] | 0.06 [0.01, 0.09] |
| 3-MBTCA | ng/m³ | 9.13 [1.75, 12.92] | 9.8 [1.83, 13.18] | 8.5 [1.72, 11.89] | 9.09 [1.69, 13.18] |
| Phthalic acid | | 3.54 [1.8, 4.02] | 3.5 [1.82, 4.13] | 3.88 [1.88, 4.68] | 3.24 [1.78, 3.82] |
| Pinic acid | | 6.61 [2.3, 7.83] | 5.36 [1.65, 7.21] | 5.25 [2.48, 6.66] | 9.22 [2.94, 11.28] |
| Al | | 62.67 [19.6, 68.7] | 62.26 [22.41, 73.59] | 65.58 [21.95, 68.43] | 60.19 [16.82, 63.54] |
| As | | 0.33 [0.14, 0.39] | 0.41 [0.16, 0.47] | 0.37 [0.17, 0.48] | 0.23 [0.11, 0.27] |
| Cd | | 0.07 [0.02, 0.09] | 0.08 [0.02, 0.1] | 0.07 [0.02, 0.09] | 0.05 [0.01, 0.06] |
| Cr | | 1.65 [0.61, 1.73] | 2.27 [0.79, 2.23] | 1.61 [0.7, 1.79] | 1.05 [0.61, 1.01] |
| Cu | | 8.5 [3.82, 9.8] | 11.59 [5.17, 13.27] | 8.79 [4.08, 10.24] | 5.09 [2.72, 6.18] |
| Fe | | 215.26 [91.41, 270.23] | 241.66 [104.95, 290.45] | 248.53 [112.83, 299.27] | 155.64 [68.3, 184.7] |
| Mn | | 9.0 [2.73, 9.36] | 11.73 [3.38, 11.77] | 7.19 [2.63, 8.31] | 8.03 [2.21, 7.09] |
| Mo | | 0.59 [0.19, 0.65] | 0.8 [0.25, 0.92] | 0.63 [0.21, 0.67] | 0.35 [0.13, 0.41] |
| Ni | | 0.91 [0.37, 1.07] | 1.18 [0.5, 1.4] | 0.92 [0.39, 1.12] | 0.63 [0.3, 0.75] |
| Pb | | 4.42 [1.52, 5.01] | 5.73 [2.0, 7.23] | 4.84 [1.72, 5.75] | 2.69 [1.15, 3.06] |
| Rb | | 0.45 [0.21, 0.58] | 0.48 [0.25, 0.6] | 0.44 [0.21, 0.57] | 0.41 [0.18, 0.58] |

| | | | | | |
|---|---|---|---|---|---|
| Sb | | 1.31 [0.33, 0.93] | 1.71 [0.46, 1.33] | 1.53 [0.4, 1.26] | 0.69 [0.22, 0.51] |
| Se | | 0.39 [0.23, 0.5] | 0.43 [0.27, 0.54] | 0.41 [0.26, 0.53] | 0.32 [0.18, 0.43] |
| Sn | | 2.26 [1.41, 2.63] | 2.6 [1.55, 3.13] | 2.45 [1.49, 2.96] | 1.73 [1.28, 2.03] |
| Ti | | 3.81 [1.6, 4.95] | 4.11 [1.8, 5.57] | 3.83 [1.68, 5.08] | 3.49 [1.38, 4.32] |
| V | | 0.48 [0.16, 0.62] | 0.51 [0.19, 0.62] | 0.52 [0.16, 0.65] | 0.42 [0.13, 0.52] |
| Zn | | 20.27 [6.09, 21.82] | 26.11 [8.18, 28.63] | 23.58 [8.69, 24.41] | 11.11 [3.64, 12.07] |

## S2. Positive Matrix Factorization (PMF)

**Table S2. Summary of tracers used to identify the $PM_{10}$ sources in the PMF analysis.**

| Identified factors | Specific tracers |
|---|---|
| Biomass burning | OC*, levoglucosan, mannosan, $K^+$, Rb, $Cl^-$ |
| Primary traffic | EC, $Ca^{2+}$, Cu, Fe, Sb, Sn |
| Nitrate-rich | $NO_3^-$, $NH_4^+$ |
| Sulfate-rich | $SO_4^{2-}$, $NH_4^+$, Se |
| Mineral dust | $Ca^{2+}$, Al, Ti, V |
| Sea/road salt | $Na^+$, $Cl^-$ |
| Aged sea salt | $Na^+$, $Mg^{2+}$ |
| Industrial | As, Cd, Cr, Mn, Mo, Ni, Pb, Zn |
| Primary biogenic | Polyols, cellulose |
| MSA-rich | MSA |
| Secondary biogenic oxidation | 3-MBTCA, pinic acid |

## S3. Various artificial neural network (ANN) architectures tested for the multilayer perceptron (MLP) analysis

**Table S3. Various tested ANN architectures and their model performance based on root mean square error (RMSE) and Pearson correlation (*r*). Note: Optimal models per site (with the lowest RMSE and highest *r*) are highlighted in bold.**

| Site | Model | Activation function | Optimization Algorithm | Learning rate | $OP_v^{DTT}$ | | $OP_v^{AA}$ | | $OP_v^{DCFH}$ | |
|---|---|---|---|---|---|---|---|---|---|---|
| | | | | | RMSE | r | RMSE | r | RMSE | r |
| Urban background (UB) | MLP1 | TanH | Scaled conjugate | N/A | **0.35** | **0.94** | 0.37 | 0.96 | 0.25 | 0.97 |
| | MLP2 | Sigmoid | Scaled conjugate | N/A | 0.36 | 0.93 | 0.35 | 0.97 | 0.21 | 0.98 |
| | MLP3 | TanH | Gradient descent | 0.2 | 0.40 | 0.92 | 0.39 | 0.96 | 0.31 | 0.95 |
| | MLP4 | TanH | Gradient descent | 0.4 | 0.36 | 0.93 | **0.32** | **0.97** | **0.19** | **0.98** |
| | MLP5 | TanH | Gradient descent | 0.6 | 0.39 | 0.92 | 0.41 | 0.96 | 0.29 | 0.96 |
| | MLP6 | Sigmoid | Gradient descent | 0.2 | 0.38 | 0.93 | 0.33 | 0.97 | 0.21 | 0.98 |
| | MLP7 | Sigmoid | Gradient descent | 0.4 | 0.38 | 0.93 | 0.36 | 0.97 | 0.22 | 0.98 |
| | MLP8 | Sigmoid | Gradient descent | 0.6 | 0.39 | 0.92 | 0.42 | 0.96 | 0.26 | 0.96 |
| Urban hyper-center (UH) | MLP1 | TanH | Scaled conjugate | N/A | 0.61 | 0.84 | 0.57 | 0.92 | 0.36 | 0.92 |
| | MLP2 | Sigmoid | Scaled conjugate | N/A | 0.61 | 0.83 | 0.54 | 0.93 | 0.32 | 0.94 |
| | MLP3 | TanH | Gradient descent | 0.2 | 0.58 | 0.85 | 0.58 | 0.92 | 0.35 | 0.92 |
| | MLP4 | TanH | Gradient descent | 0.4 | 0.58 | 0.85 | 0.57 | 0.92 | 0.35 | 0.93 |
| | MLP5 | TanH | Gradient descent | 0.6 | **0.54** | **0.88** | **0.50** | **0.94** | **0.30** | **0.95** |
| | MLP6 | Sigmoid | Gradient descent | 0.2 | 0.56 | 0.86 | 0.52 | 0.93 | 0.32 | 0.94 |
| | MLP7 | Sigmoid | Gradient descent | 0.4 | 0.60 | 0.85 | 0.53 | 0.93 | 0.34 | 0.93 |
| | MLP8 | Sigmoid | Gradient descent | 0.6 | 0.62 | 0.83 | 0.72 | 0.87 | 0.42 | 0.89 |
| Peri-urban (PU) | MLP1 | TanH | Scaled conjugate | N/A | 0.74 | 0.72 | 0.74 | 0.94 | 0.53 | 0.95 |
| | MLP2 | Sigmoid | Scaled conjugate | N/A | **0.62** | **0.75** | **0.42** | **0.97** | 0.31 | 0.96 |
| | MLP3 | TanH | Gradient descent | 0.2 | 0.61 | 0.65 | 0.61 | 0.89 | 0.36 | 0.90 |
| | MLP4 | TanH | Gradient descent | 0.4 | 0.58 | 0.71 | 0.44 | 0.96 | **0.33** | **0.96** |
| | MLP5 | TanH | Gradient descent | 0.6 | 0.66 | 0.73 | 0.82 | 0.95 | 0.51 | 0.95 |
| | MLP6 | Sigmoid | Gradient descent | 0.2 | 0.61 | 0.73 | 0.52 | 0.96 | 0.32 | 0.96 |
| | MLP7 | Sigmoid | Gradient descent | 0.4 | 0.60 | 0.71 | 0.58 | 0.96 | 0.39 | 0.96 |
| | MLP8 | Sigmoid | Gradient descent | 0.6 | 0.59 | 0.72 | 0.50 | 0.96 | 0.34 | 0.96 |

### S4. Daily distribution of $PM_{10}$ sources and observed OP activity

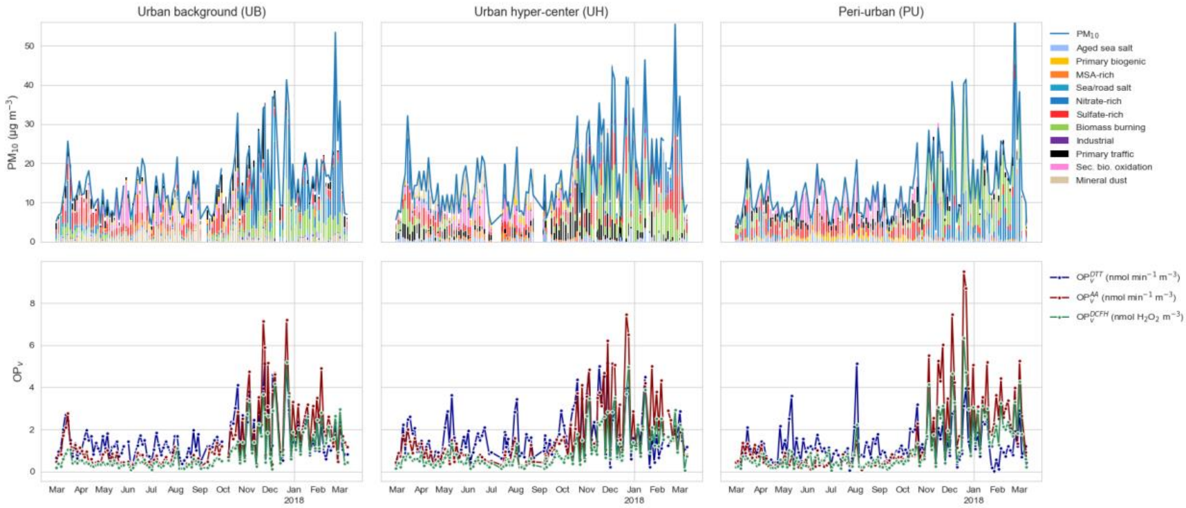


**Figure S1: Daily temporal distribution of the reconstructed $PM_{10}$ mass concentration, PMF-resolved sources, and observed OP activity ($OP_v^{DTT}, OP_v^{AA},$ and $OP_v^{DCFH}$) in the three urban sites.**

### S5. Comparison between OP assays

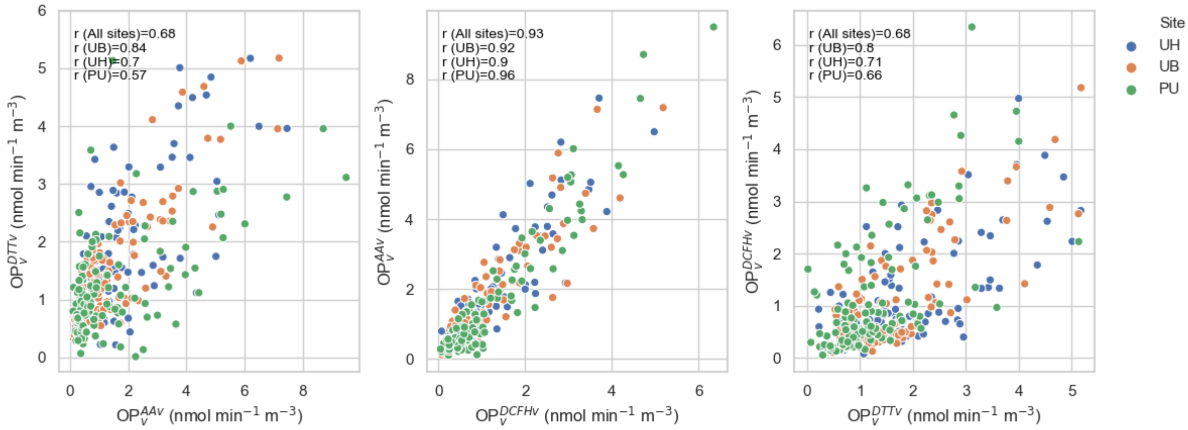


**Figure S2: Pair-wise correlation between of the OP assays (left: DTT-AA, center AA-DCFH and right DCFH-DTT). The colors refer to the sampled sites (blue: UH, orange: UB, and green: PU). Pearson *r* coefficient is given for all the sites combined and for individual sites. All correlations are significant at $p \leq 0.01$.**

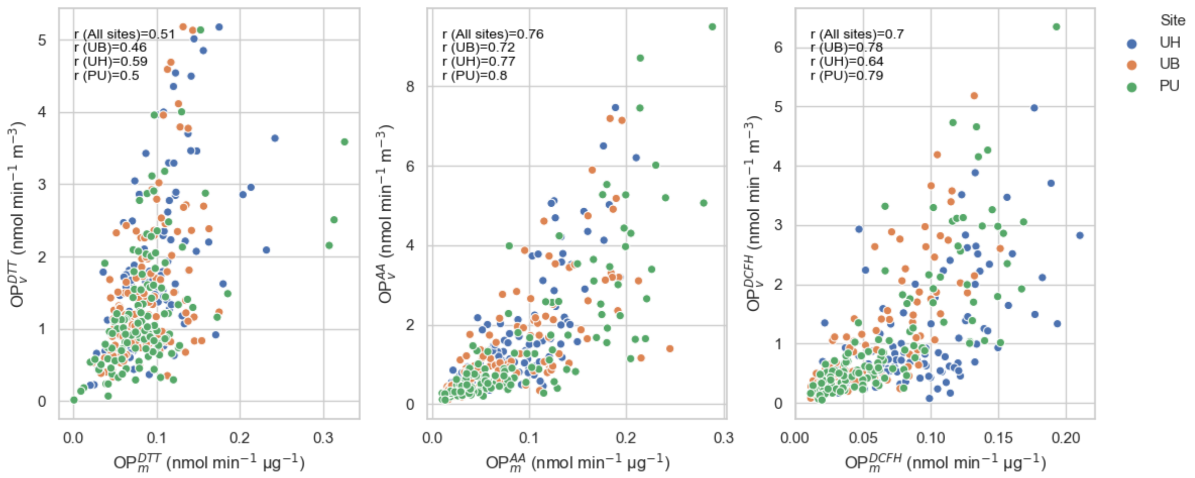


**Figure S3: Pair-wise correlation of mass- and volume-normalized OP activity ($OP_m$ and $OP_v$, respectively) for the three assays (left: DTT, center: AA, and right DCFH). The colors refer to the sampled sites (blue: UH, orange: UB and green: PU). Pearson *r* coefficient is given for all the sites combined and for individual sites. All correlations are significant at *p*≤0.01.**

## S6. Comparison of the observed and MLR-modelled OP activity

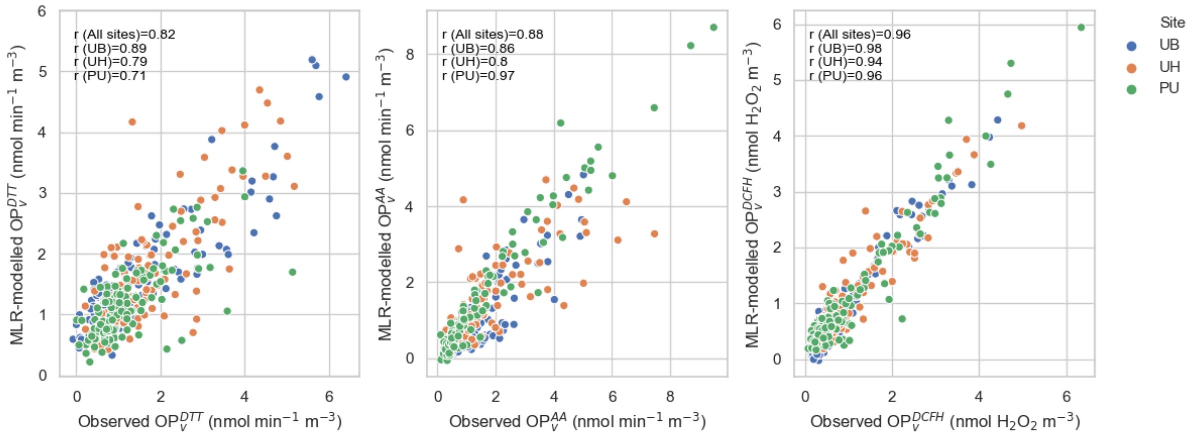


**Figure S4: Pair-wise correlation the observed and modelled volume-normalized OP activity for the three assays (left: DTT, center: AA, and right DCFH) using MLR analysis. The colors refer to the sampled sites (blue: UH, orange: UB and green: PU). Pearson *r* coefficient is given for all the sites combined and for individual sites. All correlations are significant at *p*≤0.01.**

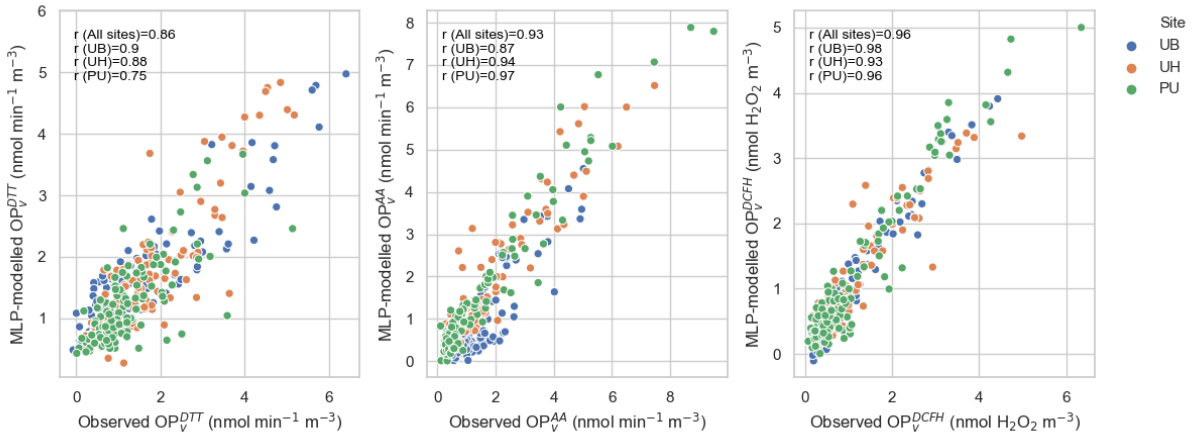

**Figure S5: Pair-wise correlation the observed and modelled volume-normalized OP activity for the three assays (left: DTT, center: AA, and right DCFH) using MLP analysis. The colors refer to the sampled sites (blue: UH, orange: UB and green: PU). Pearson *r* coefficient is given for all the sites combined and for individual sites. All correlations are significant at *p*≤0.01.**

## S7. Site-specific mean daily contribution of each source to $PM_{10}$ mass and OP activity

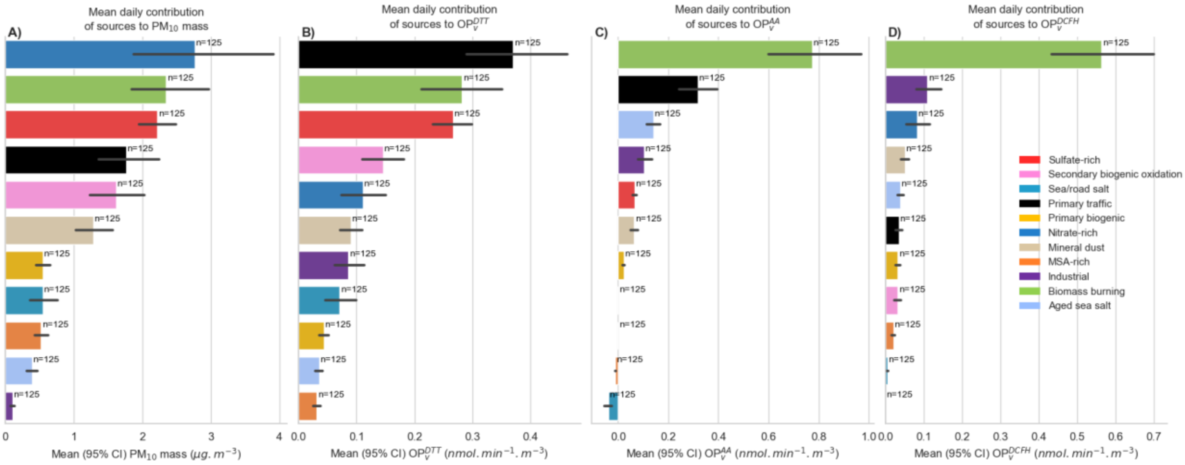


**Figure S6: Overall daily mean $OP_v$ contribution of the sources to $PM_{10}$, $OP_v^{DTT}$, $OP_v^{AA}$, and $OP_v^{DCFH}$ using MLR analysis in the UB site in the form of mean and 95% confident interval of the mean (error bar) (n=125 samples).**

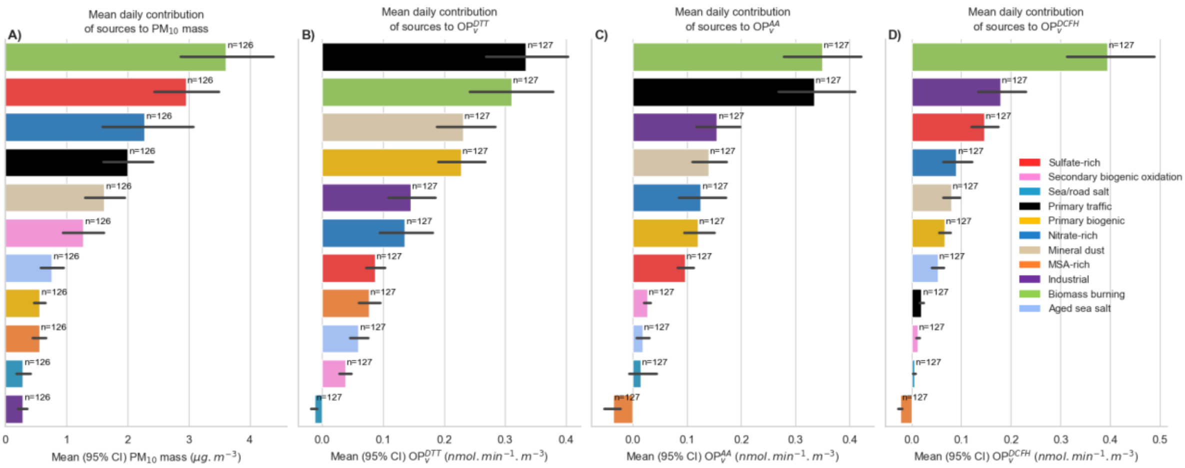


**Figure S7: Overall daily mean $OP_v$ contribution of the sources to $PM_{10}$, $OP_v^{DTT}$, $OP_v^{AA}$, and $OP_v^{DCFH}$ using MLR analysis in the UH site in the form of mean and 95% confident interval of the mean (error bar) (n=126 samples).**

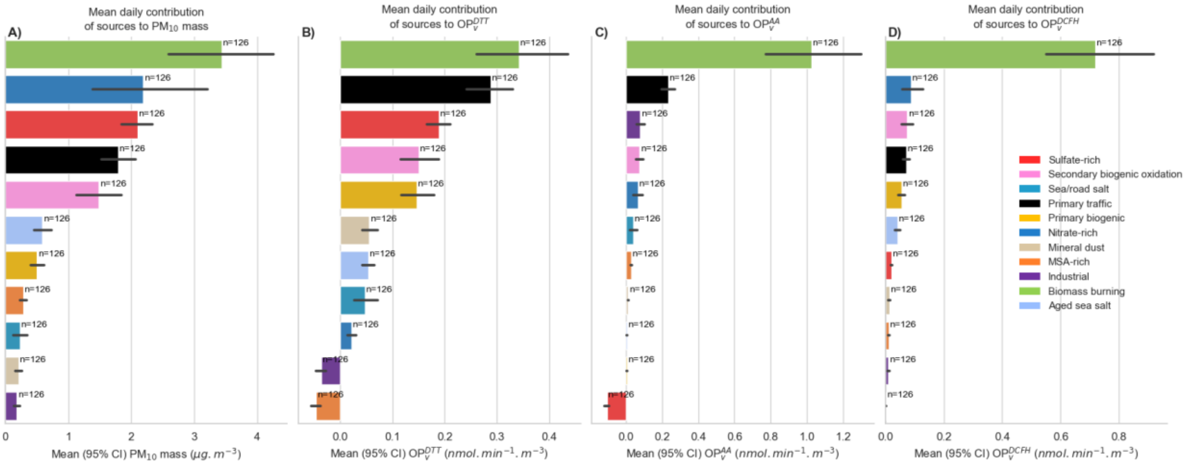


**Figure S8: Overall daily mean $OP_v$ contribution of the sources to PM10, $OP_v^{DTT}$, $OP_v^{AA}$, and $OP_v^{DCFH}$ using MLR analysis in the PU site in the form of mean and 95% confident interval of the mean (error bar) (n=126 samples).**

## S8. The non-linearity of OP contributions of $PM_{10}$ sources based on MLP analysis

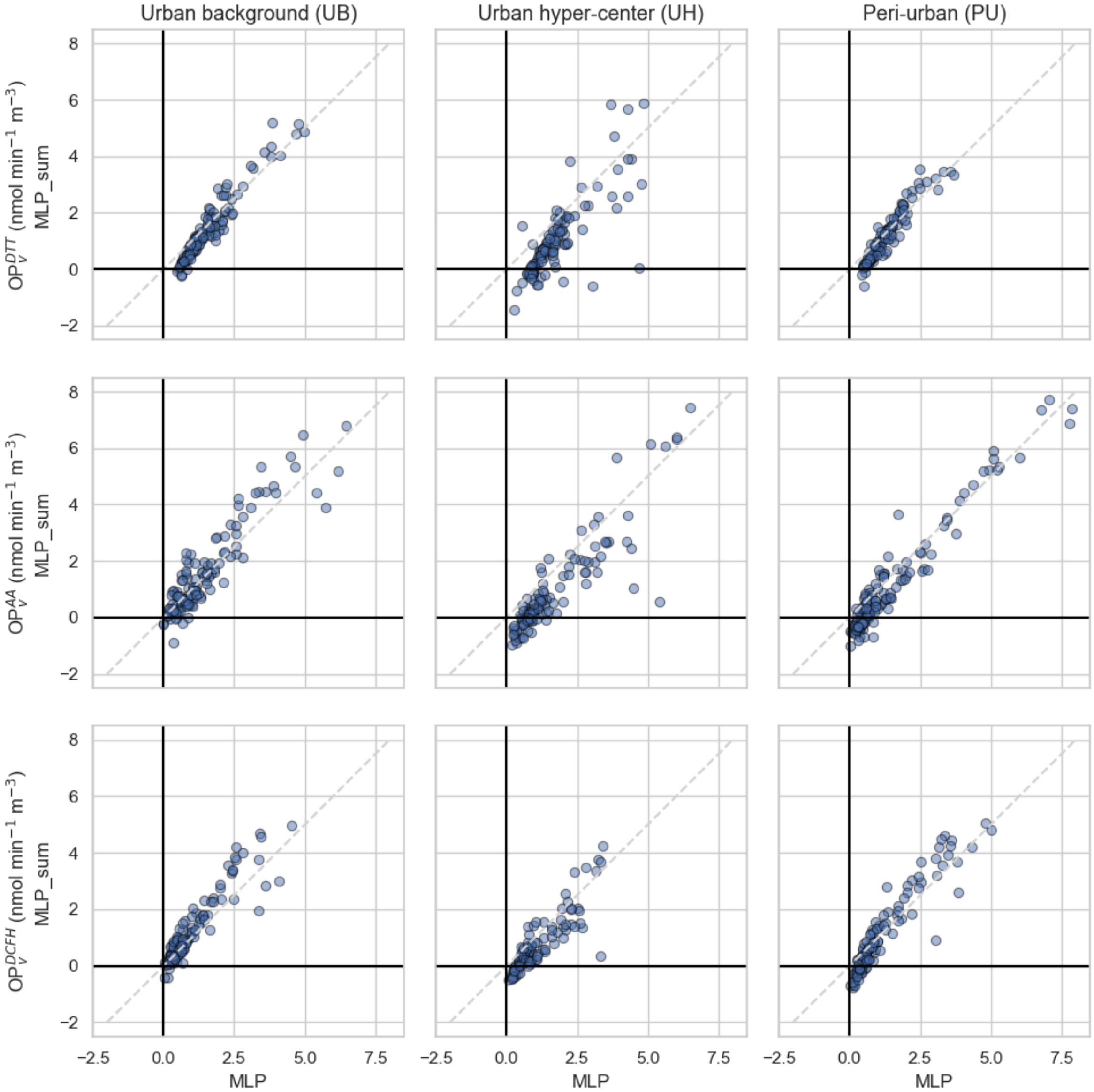


**Figure S9: The comparison of the original modelled $OP_v$ $(MLP)$ and the sum of source-specific modelled $OP_v$ activity $(MLP_{sum})$. Note: Dashed grey line corresponds to the 1:1 line. Data points below the 1:1 shows an over-all synergistic effect between $PM_{10}$ sources on OP activity, above the 1:1 line is otherwise.**

## S9. Summary of references reporting OP assays and their correlations to chemical species

**Table S4. Summary of publications relating OP assays to chemical species.**

| OP assay | Species driving responses in OP assay | Source |
|---|---|---|
| DTT | soluble nonspecific metals | (Shinyashiki et al., 2009) |
| | soluble copper | (Charrier and Anastasio, 2012, 2015; Charrier et al., 2016; Borlaza et al., 2018; Park et al., 2018; Joo et al., 2018) |
| | soluble manganese | (Charrier and Anastasio, 2012, 2015; Charrier et al., 2016; Borlaza et al., 2018; Park et al., 2018; Joo et al., 2018) |
| | OC (including WSOC and WIOC) | (Cho et al., 2005; Fang et al., 2016; Verma et al., 2012, 2015b; Jeng, 2010; Hu et al., 2008; Verma et al., 2011, 2009; Velali et al., 2016; |

| | | |
|---|---|---|
| | | Vreeland et al., 2017; Liu et al., 2014; Borlaza et al., 2018; Park et al., 2018; Joo et al., 2018) |
| | PAHs and quinones | (Cho et al., 2005; McWhinney et al., 2013; Chung et al., 2006; Totlandsdal et al., 2015) |
| | HULIS | (Verma et al., 2012, 2015b, a; Dou et al., 2015; Ma et al., 2018) |
| AA | soluble copper | (DiStefano et al., 2009; Fang et al., 2016; Visentin et al., 2016) |
| | total copper | (Janssen et al., 2014; Pant et al., 2015) |
| | total iron | (Janssen et al., 2014; Godri et al., 2010, 2011) |
| | soluble iron | (Koehler et al., 2014) |
| | total lead | (Godri et al., 2010) |
| | total zinc | (Godri et al., 2011) |
| | soluble manganese | (Visentin et al., 2016) |
| | OC | (Calas et al., 2018) |
| DCFH | soluble nonspecific metals | (DiStefano et al., 2009) |
| | soluble copper | (Charrier et al., 2014; Wang et al., 2010) |
| | soluble iron | (Wang et al., 2010) |
| | soluble zinc | (Wang et al., 2010) |
| | Quinones | (Xiong et al., 2017) |

**References**

Borlaza, L. J. S., Cosep, E. M. R., Kim, S., Lee, K., Joo, H., Park, M., Bate, D., Cayetano, M. G., and Park, K.: Oxidative potential of fine ambient particles in various environments, Environmental Pollution, 243, 1679–1688, https://doi.org/10.1016/j.envpol.2018.09.074, 2018.

Calas, A., Uzu, G., Kelly, F. J., Houdier, S., Martins, J. M. F., Thomas, F., Molton, F., Charron, A., Dunster, C., Oliete, A., Jacob, V., Besombes, J.-L., Chevrier, F., and Jaffrezo, J.-L.: Comparison between five acellular oxidative potential measurement assays performed with detailed chemistry on PM<sub>10</sub> samples from the city of Chamonix (France), Atmos. Chem. Phys., 18, 7863–7875, https://doi.org/10.5194/acp-18-7863-2018, 2018.

Charrier, J. G. and Anastasio, C.: On dithiothreitol (DTT) as a measure of oxidative potential for ambient particles: evidence for the importance of soluble transition metals, Atmos. Chem. Phys., 12, 9321–9333, https://doi.org/10.5194/acp-12-9321-2012, 2012.

Charrier, J. G. and Anastasio, C.: Rates of Hydroxyl Radical Production from Transition Metals and Quinones in a Surrogate Lung Fluid, Environ Sci Technol, 49, 9317–9325, https://doi.org/10.1021/acs.est.5b01606, 2015.

Charrier, J. G., McFall, A. S., Richards-Henderson, N. K., and Anastasio, C.: Hydrogen Peroxide Formation in a Surrogate Lung Fluid by Transition Metals and Quinones Present in Particulate Matter, Environ. Sci. Technol., 48, 7010–7017, https://doi.org/10.1021/es501011w, 2014.

Charrier, J. G., McFall, A. S., Vu, K. K.-T., Baroi, J., Olea, C., Hasson, A., and Anastasio, C.: A bias in the "mass-normalized" DTT response – An effect of non-linear concentration-response curves for copper and manganese, Atmospheric Environment, 144, 325–334, https://doi.org/10.1016/j.atmosenv.2016.08.071, 2016.

Cho, A. K., Sioutas, C., Miguel, A. H., Kumagai, Y., Schmitz, D. A., Singh, M., Eiguren-Fernandez, A., and Froines, J. R.: Redox activity of airborne particulate matter at different sites in the Los Angeles Basin, Environmental Research, 99, 40–47, https://doi.org/10.1016/j.envres.2005.01.003, 2005.

Chung, M. Y., Lazaro, R. A., Lim, D., Jackson, J., Lyon, J., Rendulic, D., and Hasson, A. S.: Aerosol-borne quinones and reactive oxygen species generation by particulate matter extracts, Environ Sci Technol, 40, 4880–4886, https://doi.org/10.1021/es0515957, 2006.

Daellenbach, K. R., Uzu, G., Jiang, J., Cassagnes, L.-E., Leni, Z., Vlachou, A., Stefenelli, G., Canonaco, F., Weber, S., Segers, A., Kuenen, J. J. P., Schaap, M., Favez, O., Albinet, A., Aksoyoglu, S., Dommen, J., Baltensperger, U., Geiser, M., El Haddad, I., Jaffrezo, J.-L., and Prévôt, A. S. H.: Sources of particulate-matter air pollution and its oxidative potential in Europe, Nature, 587, 414–419, https://doi.org/10.1038/s41586-020-2902-8, 2020.

DiStefano, E., Eiguren-Fernandez, A., Delfino, R. J., Sioutas, C., Froines, J. R., and Cho, A. K.: Determination of metal-based hydroxyl radical generating capacity of ambient and diesel exhaust particles, Inhal Toxicol, 21, 731–738, https://doi.org/10.1080/08958370802491433, 2009.

Dou, J., Lin, P., Kuang, B.-Y., and Yu, J. Z.: Reactive Oxygen Species Production Mediated by Humic-like Substances in Atmospheric Aerosols: Enhancement Effects by Pyridine, Imidazole, and Their Derivatives, Environ. Sci. Technol., 49, 6457–6465, https://doi.org/10.1021/es5059378, 2015.

Fang, T., Verma, V., Bates, J. T., Abrams, J., Klein, M., Strickland, M. J., Sarnat, S. E., Chang, H. H., Mulholland, J. A., Tolbert, P. E., Russell, A. G., and Weber, R. J.: Oxidative potential of ambient water-soluble $PM_{2.5}$ in the southeastern United States: contrasts in sources and health associations between ascorbic acid (AA) and dithiothreitol (DTT) assays, Atmos. Chem. Phys., 16, 3865–3879, https://doi.org/10.5194/acp-16-3865-2016, 2016.

Godri, K. J., Duggan, S. T., Fuller, G. W., Baker, T., Green, D., Kelly, F. J., and Mudway, I. S.: Particulate matter oxidative potential from waste transfer station activity, Environ Health Perspect, 118, 493–498, https://doi.org/10.1289/ehp.0901303, 2010.

Godri, K. J., Harrison, R. M., Evans, T., Baker, T., Dunster, C., Mudway, I. S., and Kelly, F. J.: Increased oxidative burden associated with traffic component of ambient particulate matter at roadside and urban background schools sites in London, PLoS One, 6, e21961, https://doi.org/10.1371/journal.pone.0021961, 2011.

Hu, S., Polidori, A., Arhami, M., Shafer, M. M., Schauer, J. J., Cho, A., and Sioutas, C.: Redox activity and chemical speciation of size fractioned PM in the communities of the Los Angeles – Long Beach Harbor, https://doi.org/10.5194/acpd-8-11643-2008, 2008.

Janssen, N. A. H., Yang, A., Strak, M., Steenhof, M., Hellack, B., Gerlofs-Nijland, M. E., Kuhlbusch, T., Kelly, F., Harrison, R., Brunekreef, B., Hoek, G., and Cassee, F.: Oxidative potential of particulate matter collected at sites with different source characteristics, Science of The Total Environment, 472, 572–581, https://doi.org/10.1016/j.scitotenv.2013.11.099, 2014.

Jeng, H. A.: Chemical composition of ambient particulate matter and redox activity, Environ Monit Assess, 169, 597–606, https://doi.org/10.1007/s10661-009-1199-8, 2010.

Joo, H. S., Batmunkh, T., Borlaza, L. J. S., Park, M., Lee, K. Y., Lee, J. Y., Chang, Y. W., and Park, K.: Physicochemical properties and oxidative potential of fine particles produced from coal combustion, Aerosol Science and Technology, 52, 1134–1144, https://doi.org/10.1080/02786826.2018.1501152, 2018.

Koehler, K., Shapiro, J., Sameenoi, Y., Henry, C., and Volckens, J.: LABORATORY EVALUATION OF A MICROFLUIDIC ELECTROCHEMICAL SENSOR FOR AEROSOL OXIDATIVE LOAD, Aerosol Sci Technol, 48, 489–497, https://doi.org/10.1080/02786826.2014.891722, 2014.

Leni, Z., Cassagnes, L. E., Daellenbach, K. R., El Haddad, I., Vlachou, A., Uzu, G., Prévôt, A. S. H., Jaffrezo, J.-L., Baumlin, N., Salathe, M., Baltensperger, U., Dommen, J., and Geiser, M.: Oxidative stress-induced inflammation in susceptible airways by anthropogenic aerosol, PLoS ONE, 15, e0233425, https://doi.org/10.1371/journal.pone.0233425, 2020.

Liu, Q., Zhang, Y., Liu, Y., and Zhang, M.: Characterization of springtime airborne particulate matter-bound reactive oxygen species in Beijing, Environ Sci Pollut Res, 21, 9325–9333, https://doi.org/10.1007/s11356-014-2843-6, 2014.

Ma, Y., Cheng, Y., Qiu, X., Cao, G., Fang, Y., Wang, J., Zhu, T., Yu, J., and Hu, D.: Sources and oxidative potential of water-soluble humic-like substances (HULIS<sub>WS</sub>) in fine particulate matter (PM<sub>2.5</sub>) in Beijing, Atmos. Chem. Phys., 18, 5607–5617, https://doi.org/10.5194/acp-18-5607-2018, 2018.

McWhinney, R. D., Badali, K., Liggio, J., Li, S.-M., and Abbatt, J. P. D.: Filterable redox cycling activity: a comparison between diesel exhaust particles and secondary organic aerosol constituents, Environ Sci Technol, 47, 3362–3369, https://doi.org/10.1021/es304676x, 2013.

Pant, P., Baker, S. J., Shukla, A., Maikawa, C., Godri Pollitt, K. J., and Harrison, R. M.: The PM 10 fraction of road dust in the UK and India: Characterization, source profiles and oxidative potential, Science of The Total Environment, 530–531, 445–452, https://doi.org/10.1016/j.scitotenv.2015.05.084, 2015.

Park, M., Joo, H. S., Lee, K., Jang, M., Kim, S. D., Kim, I., Borlaza, L. J. S., Lim, H., Shin, H., Chung, K. H., Choi, Y.-H., Park, S. G., Bae, M.-S., Lee, J., Song, H., and Park, K.: Differential toxicities of fine particulate matters from various sources, Sci Rep, 8, 17007, https://doi.org/10.1038/s41598-018-35398-0, 2018.

Samake, A., Uzu, G., Martins, J. M. F., Calas, A., Vince, E., Parat, S., and Jaffrezo, J. L.: The unexpected role of bioaerosols in the Oxidative Potential of PM, 7, 10978, https://doi.org/10.1038/s41598-017-11178-0, 2017.

Shinyashiki, M., Eiguren-Fernandez, A., Schmitz, D. A., Di Stefano, E., Li, N., Linak, W. P., Cho, S.-H., Froines, J. R., and Cho, A. K.: Electrophilic and redox properties of diesel exhaust particles, Environ Res, 109, 239–244, https://doi.org/10.1016/j.envres.2008.12.008, 2009.

Totlandsdal, A. I., Låg, M., Lilleaas, E., Cassee, F., and Schwarze, P.: Differential proinflammatory responses induced by diesel exhaust particles with contrasting PAH and metal content, Environ Toxicol, 30, 188–196, https://doi.org/10.1002/tox.21884, 2015.

Velali, E., Papachristou, E., Pantazaki, A., Choli-Papadopoulou, T., Planou, S., Kouras, A., Manoli, E., Besis, A., Voutsa, D., and Samara, C.: Redox activity and in vitro bioactivity of the water-soluble fraction of urban particulate matter in relation to particle size and chemical composition, Environmental Pollution, 208, 774–786, https://doi.org/10.1016/j.envpol.2015.10.058, 2016.

Verma, V., Ning, Z., Cho, A. K., Schauer, J. J., Shafer, M. M., and Sioutas, C.: Redox activity of urban quasi-ultrafine particles from primary and secondary sources, Atmospheric Environment, 43, 6360–6368, https://doi.org/10.1016/j.atmosenv.2009.09.019, 2009.

Verma, V., Pakbin, P., Cheung, K. L., Cho, A. K., Schauer, J. J., Shafer, M. M., Kleinman, M. T., and Sioutas, C.: Physicochemical and oxidative characteristics of semi-volatile components of quasi-ultrafine particles in an urban atmosphere, Atmospheric Environment, 45, 1025–1033, https://doi.org/10.1016/j.atmosenv.2010.10.044, 2011.

Verma, V., Rico-Martinez, R., Kotra, N., King, L., Liu, J., Snell, T. W., and Weber, R. J.: Contribution of Water-Soluble and Insoluble Components and Their Hydrophobic/Hydrophilic Subfractions to the Reactive Oxygen Species-Generating Potential of Fine Ambient Aerosols, Environ. Sci. Technol., 46, 11384–11392, https://doi.org/10.1021/es302484r, 2012.

Verma, V., Wang, Y., El-Afifi, R., Fang, T., Rowland, J., Russell, A. G., and Weber, R. J.: Fractionating ambient humic-like substances (HULIS) for their reactive oxygen species activity – Assessing the importance of quinones and atmospheric aging, Atmospheric Environment, 120, 351–359, https://doi.org/10.1016/j.atmosenv.2015.09.010, 2015a.

Verma, V., Fang, T., Xu, L., Peltier, R. E., Russell, A. G., Ng, N. L., and Weber, R. J.: Organic Aerosols Associated with the Generation of Reactive Oxygen Species (ROS) by Water-Soluble $PM_{2.5}$, Environ. Sci. Technol., 49, 4646–4656, https://doi.org/10.1021/es505577w, 2015b.

Visentin, M., Pagnoni, A., Sarti, E., and Pietrogrande, M. C.: Urban PM2.5 oxidative potential: Importance of chemical species and comparison of two spectrophotometric cell-free assays, Environmental Pollution, 219, 72–79, https://doi.org/10.1016/j.envpol.2016.09.047, 2016.

Vreeland, H., Weber, R., Bergin, M., Greenwald, R., Golan, R., Russell, A. G., Verma, V., and Sarnat, J. A.: Oxidative potential of PM 2.5 during Atlanta rush hour: Measurements of in-vehicle dithiothreitol (DTT) activity, Atmospheric Environment, 165, 169–178, https://doi.org/10.1016/j.atmosenv.2017.06.044, 2017.

Wang, Y., Arellanes, C., Curtis, D. B., and Paulson, S. E.: Probing the source of hydrogen peroxide associated with coarse mode aerosol particles in southern California, Environ Sci Technol, 44, 4070–4075, https://doi.org/10.1021/es100593k, 2010.

Xiong, Q., Yu, H., Wang, R., Wei, J., and Verma, V.: Rethinking Dithiothreitol-Based Particulate Matter Oxidative Potential: Measuring Dithiothreitol Consumption versus Reactive Oxygen Species Generation, Environ. Sci. Technol., 51, 6507–6514, https://doi.org/10.1021/acs.est.7b01272, 2017.

Yu, H., Wei, J., Cheng, Y., Subedi, K., and Verma, V.: Synergistic and Antagonistic Interactions among the Particulate Matter Components in Generating Reactive Oxygen Species Based on the Dithiothreitol Assay, Environ. Sci. Technol., 52, 2261–2270, https://doi.org/10.1021/acs.est.7b04261, 2018.